Supplementary Figures, Legends, and Tables.

Figure S1

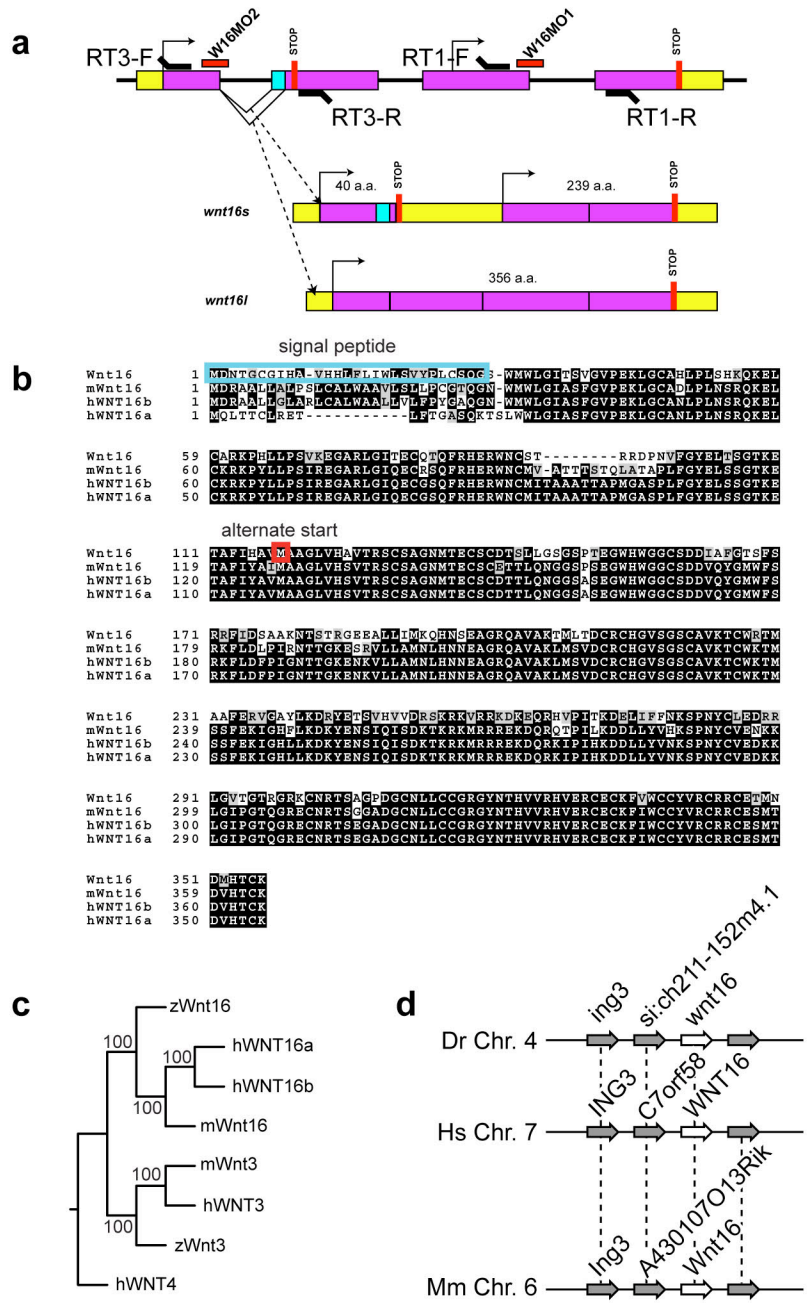

Supplementary Figure 1. Characterization of the zebrafish *wnt16* orthologue. a) Genomic structure of the zebrafish *wnt16* locus and mRNA splice variants, with 5'- and 3'-UTR (yellow) and open reading frames (ORFs; purple) found on four exons (top). Locations of the splice junctions blocked by W16MO1 and W16MO2 are indicated, as are locations of RT-PCR primers described in the text. Alternative splice acceptors are found 52 bps apart (blue box) in the second exon. Splicing to the 5'-acceptor yields two ORFs (middle, *wnt16s*): a highly truncated 5'-ORF that encodes a peptide of 40 amino acids, and a downstream ORF encoding a short-form protein of 239 amino acids, lacking a putative signal peptide, that exhibits no biological activity when injected (Fig. S2). Splicing to the more 3'-splice acceptor results in a message (bottom, *wnt16l*) with an ORF encoding a

predicted protein of 356 amino acids that has biological activity when injected (Fig. S3); high homology to mouse Wnt16, as well as human WNT16a and WNT16b (b); and a predicted signal peptide (boxed in turquoise). c) Phylogenetic cosegregation of zebrafish Wnt16 with mammalian Wnt16 proteins, as determined using PHYLIP software and bootstrap analysis (100 replicates) using the Neighbor-Joining distance method. d) Conservation of synteny between zebrafish *wnt16* (top), human *WNT16* (middle), and mouse *Wnt16* (bottom). Schematic of relevant chromosomal regions with dashed lines linking homologous genes. Zebrafish *si:ch211-152m4.1*, human *C7orf58*, and mouse *A430107O13Rik* are homologous genes with different Ensembl annotations.

Figure S2

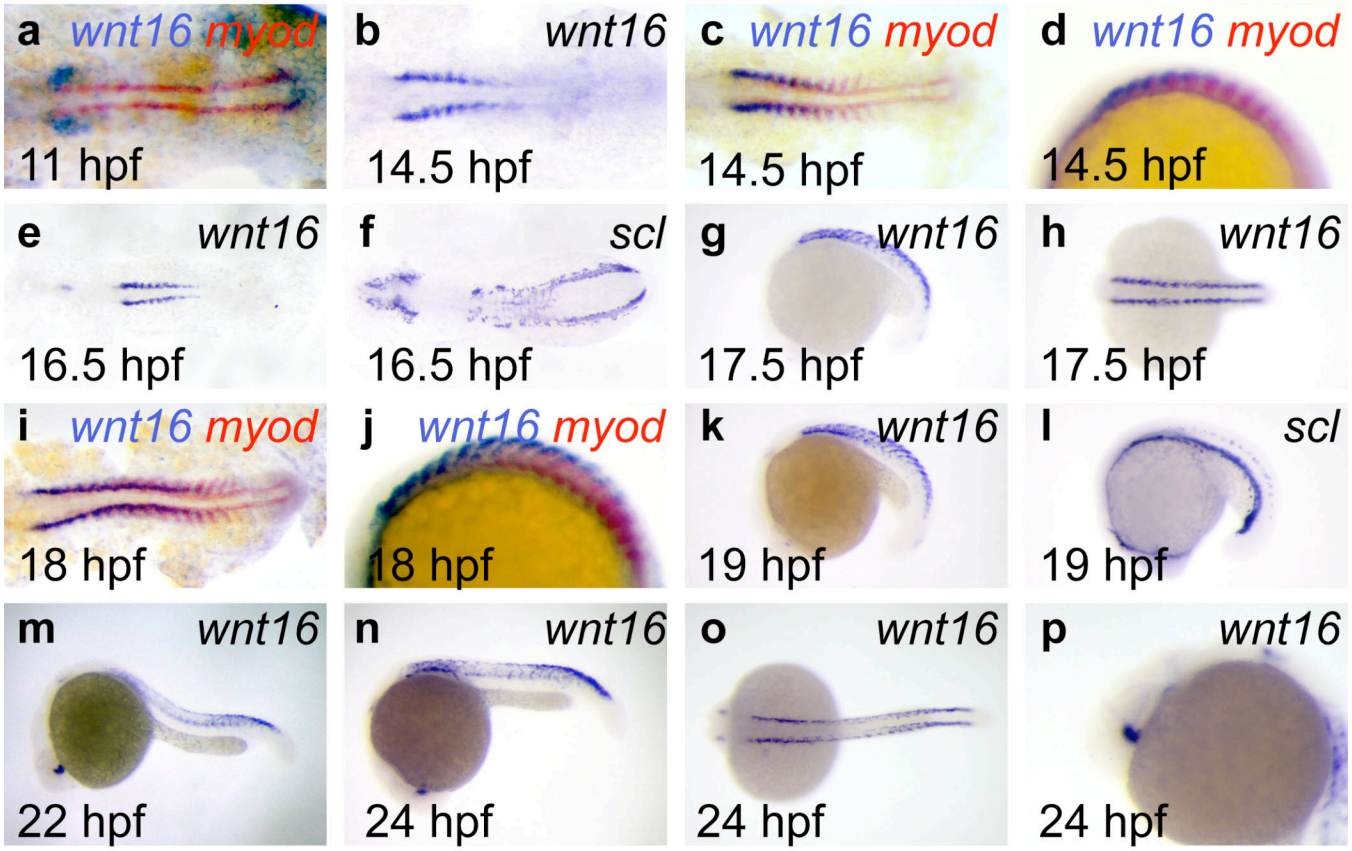

Supplementary Figure 2. Expression of zebrafish *wnt16*. Expression of *wnt16* by WISH at the embryonic stages indicated (a-e, g-k, m-p), with, in some cases, secondary processing for *myod* (red; a, c, d, i, j) to identify the location of the posterior somite compartment, and individual panels of the vascular/haematopoietic marker *scl* (f, l) for comparison. Flat mount (a-c, e-f, i), close up lateral trunk (d, j) or head (p), lateral (g, k-n), and dorsal (h, o) views are shown with anterior to the left.

Figure S3

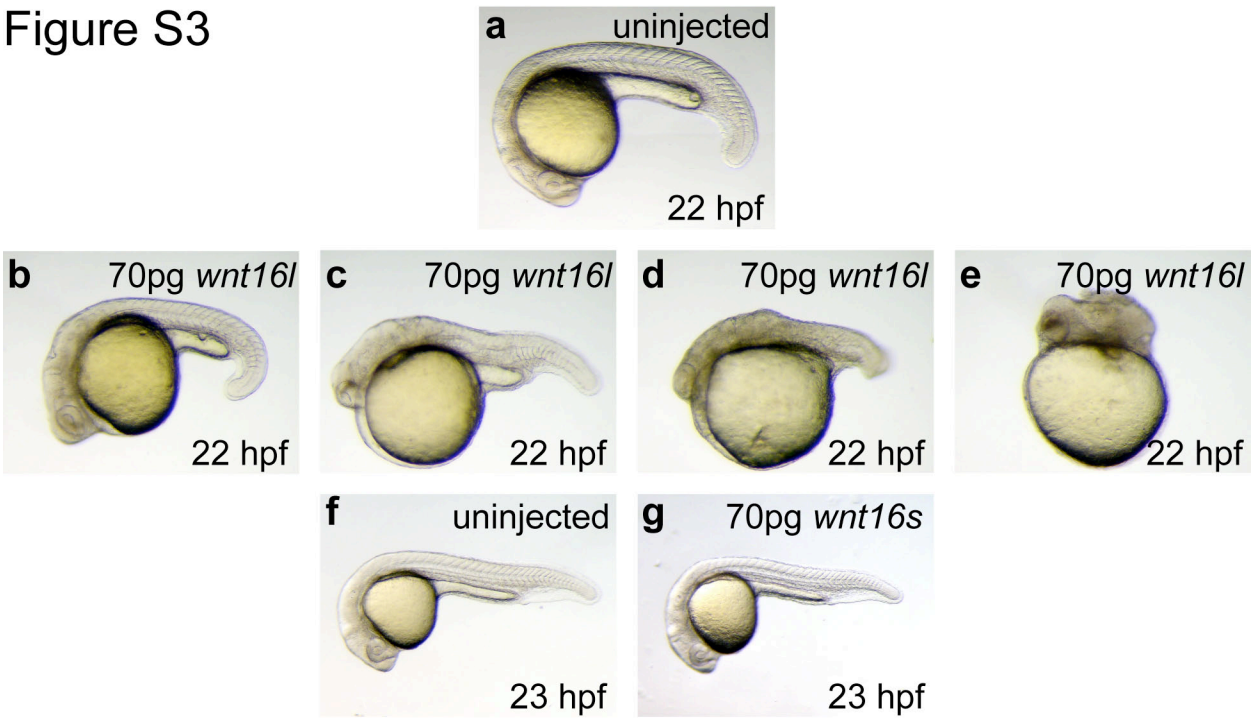

Supplementary Figure 3. Phenotypes caused by injection of *wnt16* mRNA. A representative uninjected embryo (a) at 22 hpf (26-ss) compared to sibling embryos displaying a range of phenotypes (b-e) caused by injection of 70 pg *wnt16l* isoform mRNA. A representative uninjected embryo at 23 hpf (f) compared to a representative embryo injected with 70 pg *wnt16s* isoform mRNA (g).

Figure S4

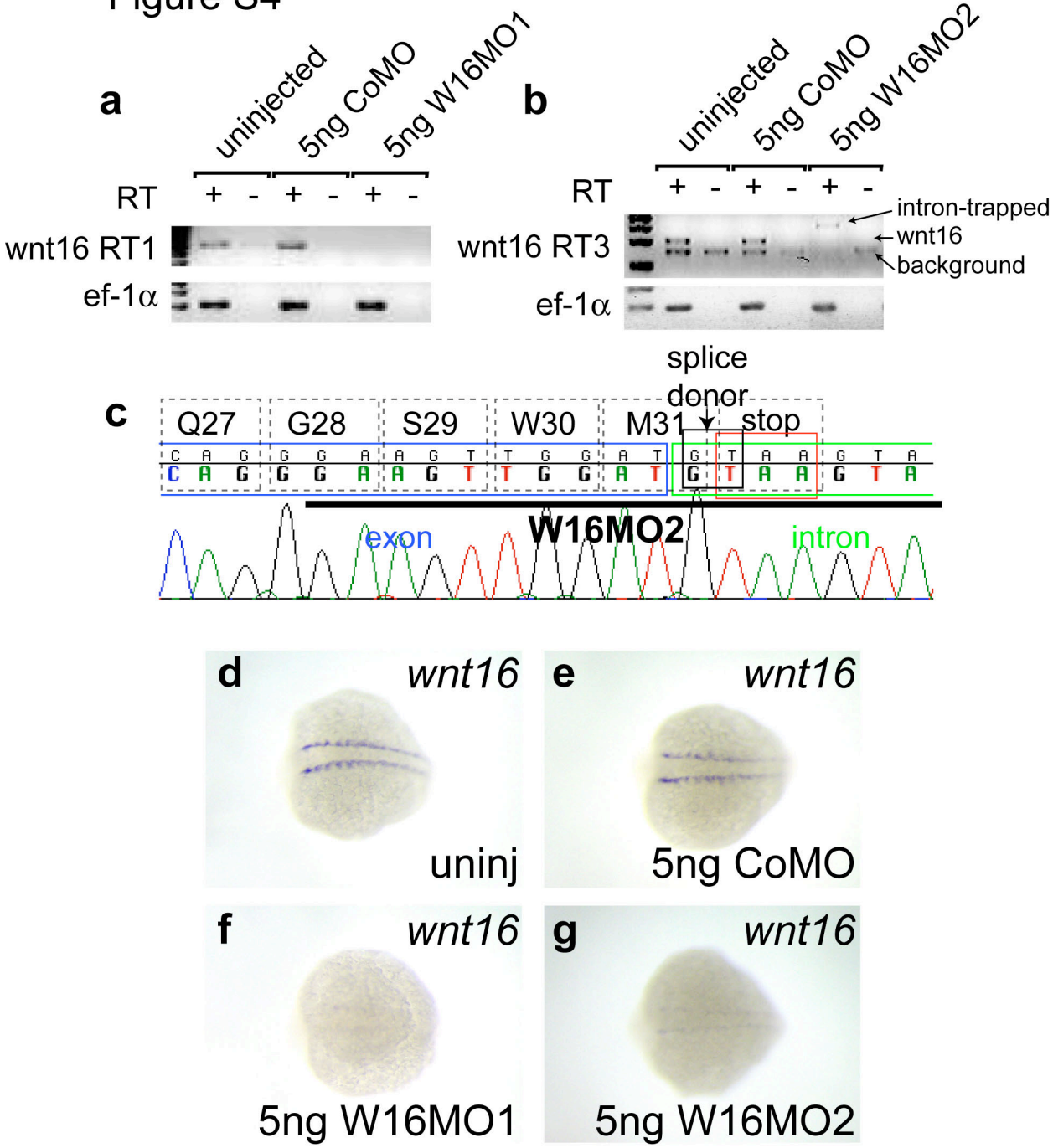

Supplementary Figure 4. Effectiveness of *wnt16* morpholinos. cDNA from embryos injected with W16MO1 (a) or W16MO2 (b) was subjected to RT-PCR analysis using RT1 (a) or RT3 (b) primers depicted in Fig. S1, and *ef-1α* as a control. For W16MO1 no higher molecular weight products were observed, indicating that message was degraded by nonsense-mediated decay. The intron-trapped product (indicated, b) produced by W16MO2 injection, was verified by sequencing and leads to message with an introduced stop codon after amino acid 31 (c). WISH demonstrates that the *wnt16* transcript recognized by the wild-type probe is present at normal levels in uninjected embryos (278/278; d) and embryos injected with a control 5-base-mismatch morpholino (124/124; e), but not embryos injected with W16MO1 (181/215; f) or W16MO2 (130/147; g). d-g, 17 hpf (16-ss) embryos, dorsal views, with anterior to the left.

Figure S5

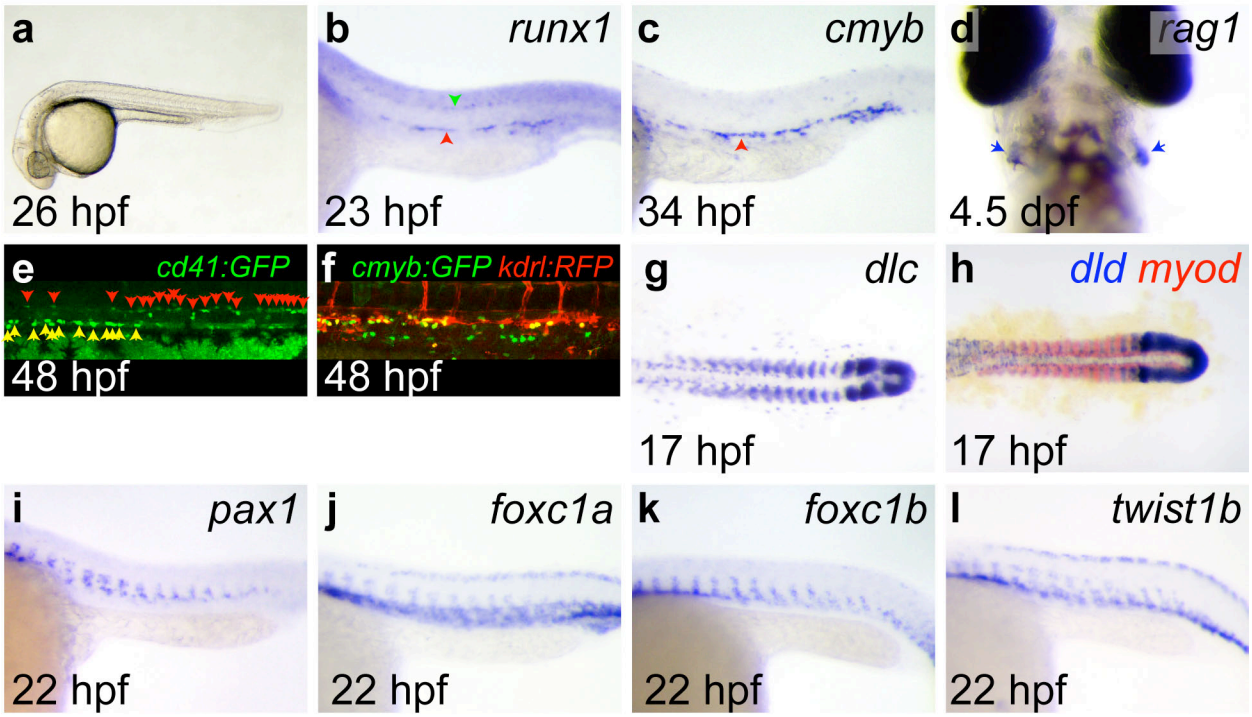

Supplementary Figure 5. Wnt16 control morpholino effects. Embryos injected with 5ng of a control morpholino with 5 bp mismatches compared to W16MO1 have unaffected Wnt16-regulated gene expression. Brightfield (a), *runx1* (b), *cmyb* (c), *rag1* (d), *cd41:GFP* (e), *cmyb:GFP;kdrl:RFP* (f), *dlc* (g), *dld*/*myod* (h), *pax1* (i), *foxc1a* (j), *foxc1b* (k), *twist1b* (l). Red arrowheads mark dorsal aorta (b, c), or HSCs (e). Green arrowhead marks neural expression (b). Yellow arrows mark pronephric multiciliate cells (e). Blue arrows mark thymi (d). a, lateral; b, c, e, f, i-l close up lateral of trunk/aorta region; d, ventral; and g, h, flat mount. a-c, e-l anterior left; d, anterior up.

Figure S6

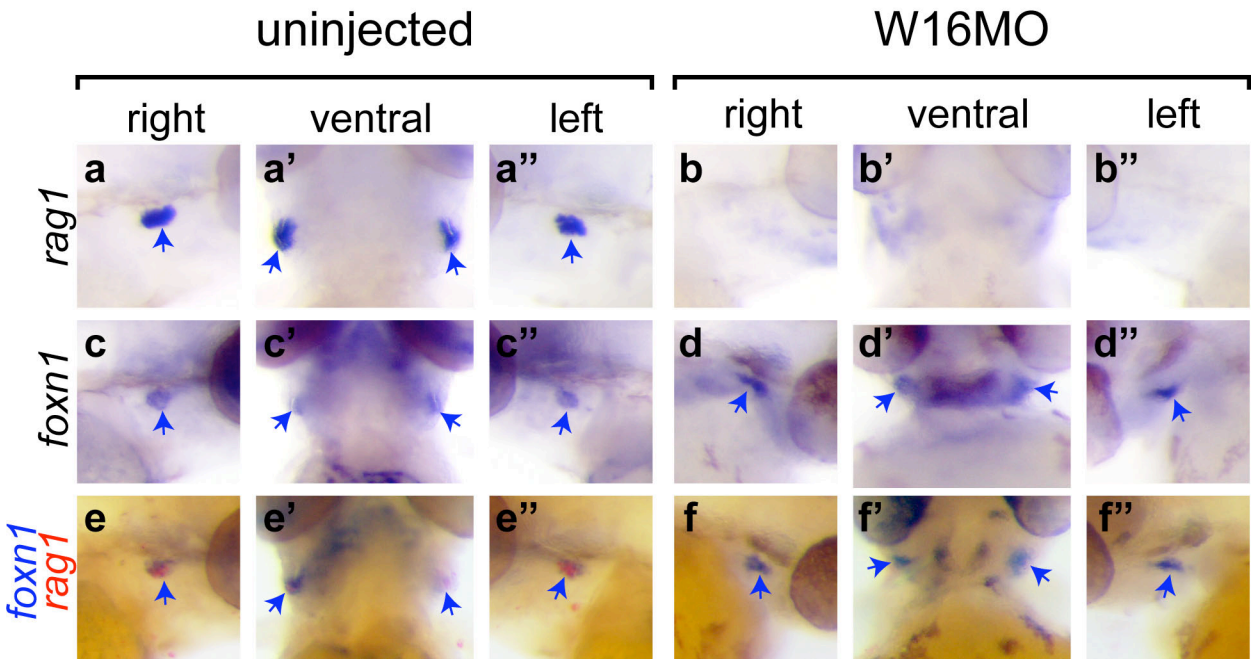

Supplementary Figure 6. Thymic epithelium is intact in W16MO animals. Expression of the lymphocyte marker *rag1* (a-b''), the thymic epithelium marker *foxn1* (c-d''), or both (e-f'') in uninjected (left panels) or W16MO-injected animals (right panels) as indicated. Right (a-f) and left (a''-f'') lateral views and ventral (a'-f') views are shown. Blue arrowheads indicate T-cells (a-a'', e-f'') and/or thymi (c-f'').

Figure S7

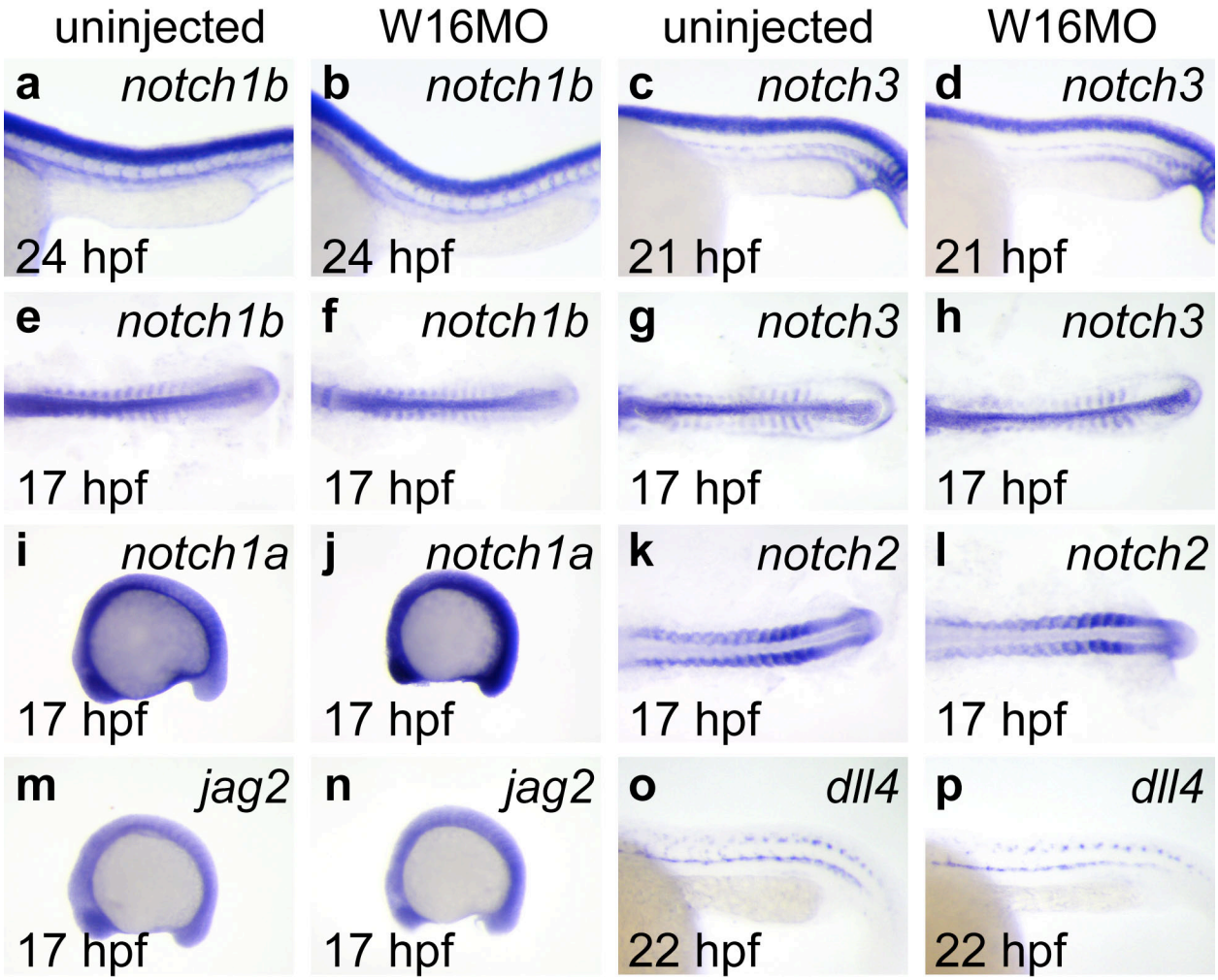

Supplementary Figure 7. Selected Notch ligands and receptors unaffected by reduction of Wnt16 activity. Comparison of the expression of *notch1b* (a-b, e-f), *notch3* (c-d, g-h), *notch1a* (i-j) *notch2* (k-l), *jag2* (m-n) and *dll4* (o-p) at the times indicated, in uninjected or W16MO-injected embryos, as indicated above each column. a-d, i-j, m-p, lateral views. g-h, k-l flat mounts. All anterior to the left.

Figure S8

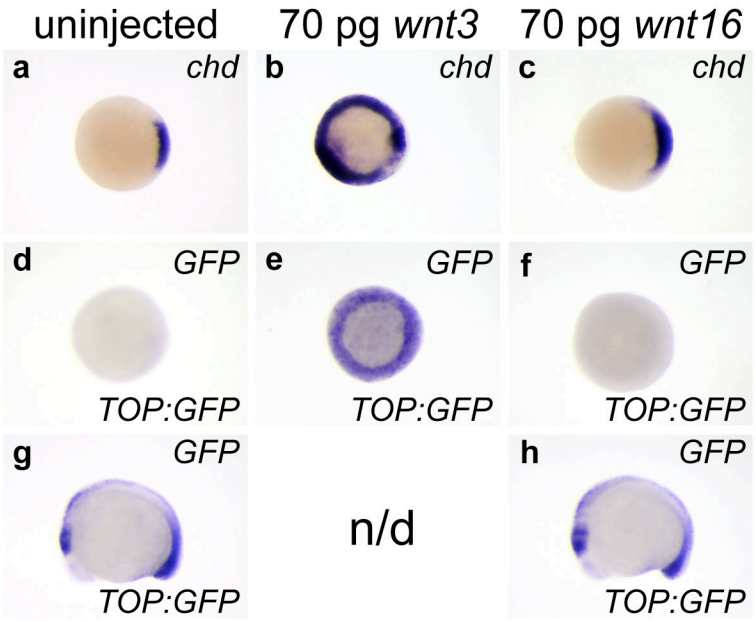

Supplementary Figure 8. Wnt16 is non-canonical. 6 hpf (shield stage; top two rows) or 17 hpf (16-ss; bottom row) embryos. Uninjected (left column), injected with 70 pg *wnt3* mRNA (center column), or 70 pg *wnt16* mRNA (right column) embryos, processed by WISH for the canonical target gene *chd* (top row), or *GFP* in *Tg(TOP:GFP)*^{w25} Wnt/β-catenin/Tcf-reporter animals (bottom two rows). a-f, animal views, dorsal to the right, where known. g-h, anterior left, dorsal up.

Figure S9

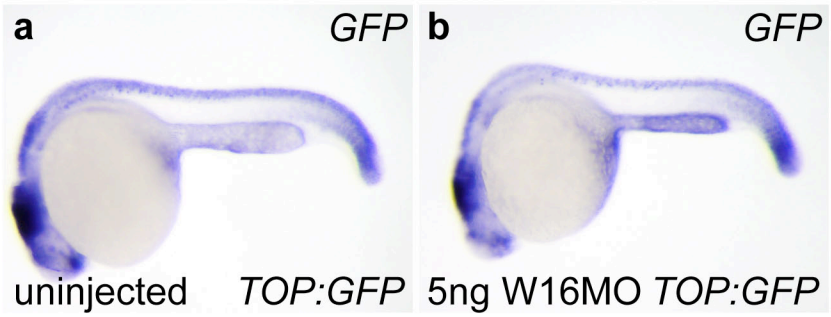

Supplementary Figure 9. Decreased Wnt16 activity does not alter β-catenin/Tcf-dependent Wnt pathway activity. Uninjected (a) or W16MO-injected (b) *Tg(TOP:GFP)*^{w25} animals processed by WISH for *GFP* show no difference in tissue-specific levels of β-catenin/Tcf-dependent Wnt signalling at 22 hpf.

Figure S10

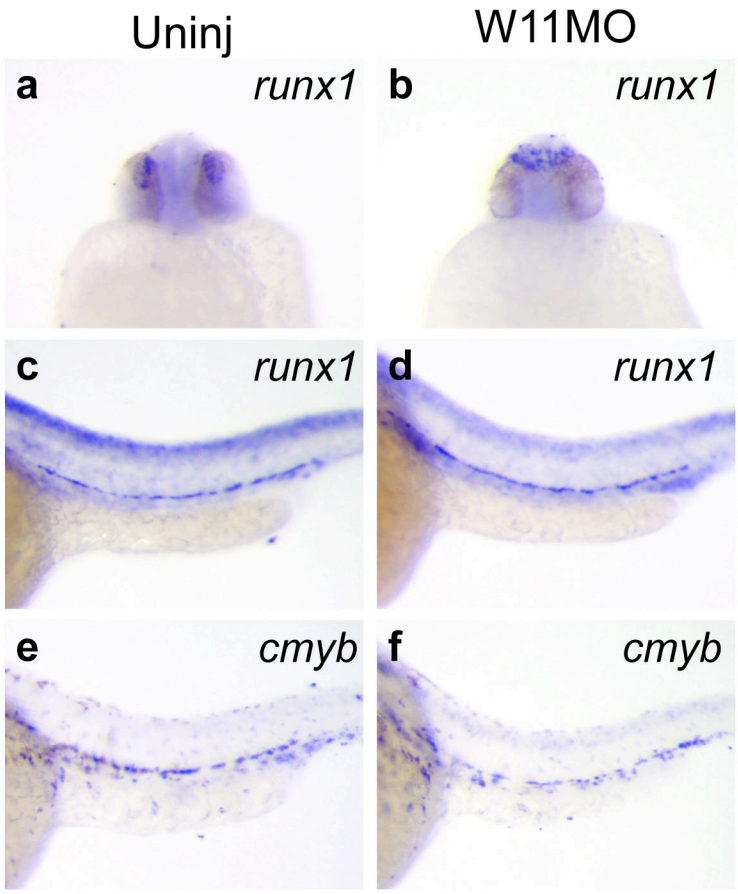

Supplementary Figure 10. Wnt11 knock down does not affect HSCs. Wild-type (a) or cyclopic phenotype (b) confirms Wnt11 knockdown. Embryos processed for the HSC markers *runx1* at 24 hpf (c-d) or *cmyb* at 36 hpf (e-f). Uninjected (left column) or W11MO-injected (right column). a-b, ventral head views. c-f close up lateral trunk views, anterior left.

Figure S11

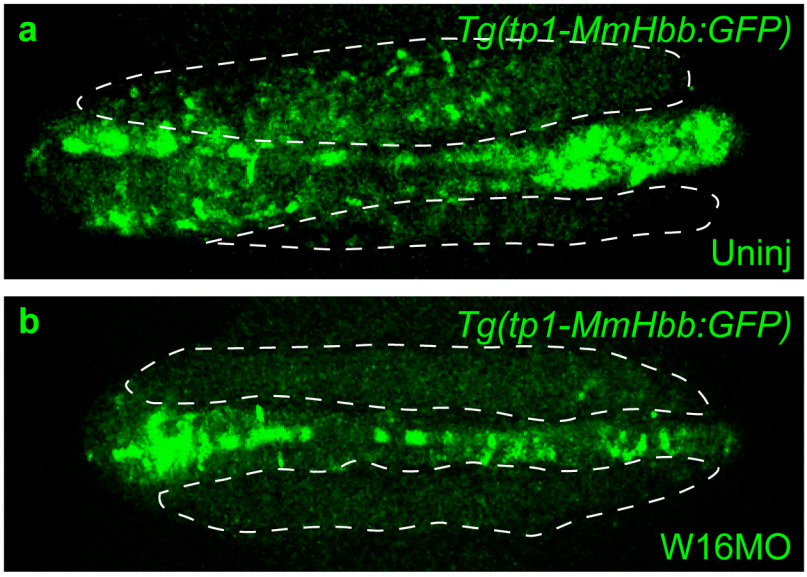

Supplementary Figure 11. Decreased expression of a Notch reporter fluorophore in W16MO somites. GFP fluorescence in the somites (outlined with dashed white lines) and axial tissue of a transgenic animal carrying *gfp* under the control of a Notch-responsive promoter was examined by max-projection confocal imaging at 17.5 hpf in uninjected (a) or W16MO-injected (b) animals. Dorsal views, anterior left.

Figure S12

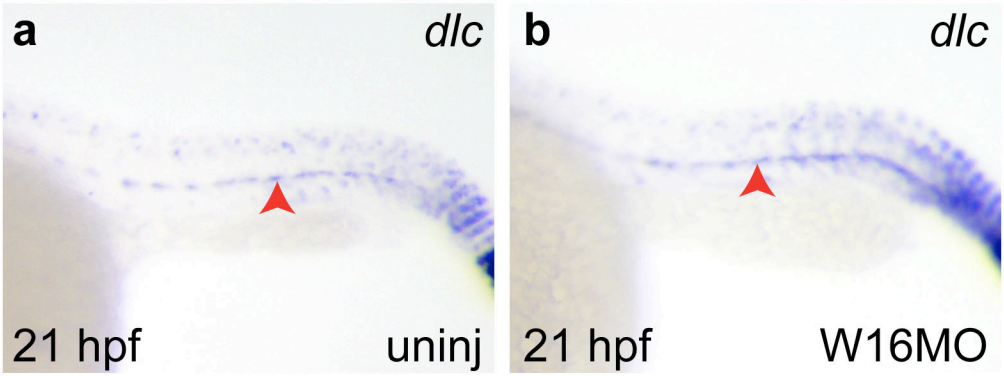

Supplementary Figure 12. Dorsal aorta expression of *dlc* in *wnt16* morphants. Comparative expression of *dlc* in the dorsal aorta (red arrowhead) of uninjected (a) or W16MO-injected (b) embryos at 21 hpf (24-ss). Close up lateral views, anterior to the left.

Figure S13

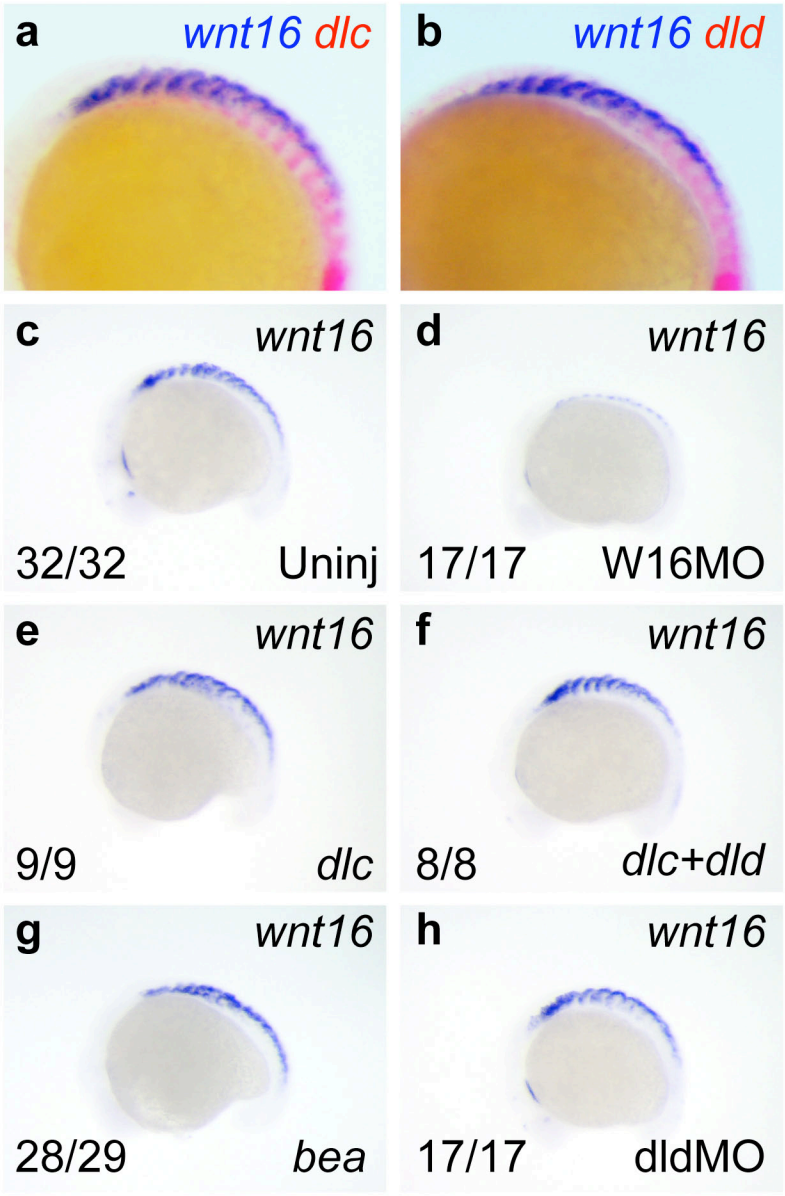

Supplementary Figure 13. Dlc/Dld do not regulate *wnt16*. Expression of *wnt16* at 17 hpf (16-ss) was compared to that of *dlc* (a) or *dld* (b) to examine overlap. Both overlapping and non-overlapping expression is observed. *Wnt16* expression in uninjected (c), W16MO-injected (d), *dlc* mRNA-injected (e), *dlc+dld* mRNA-injected (f), *bea* homozygous mutants (g), and *dld*MO-injected animals (h). Only W16MO causes an alteration in *wnt16*. All lateral views, anterior left.

Figure S14

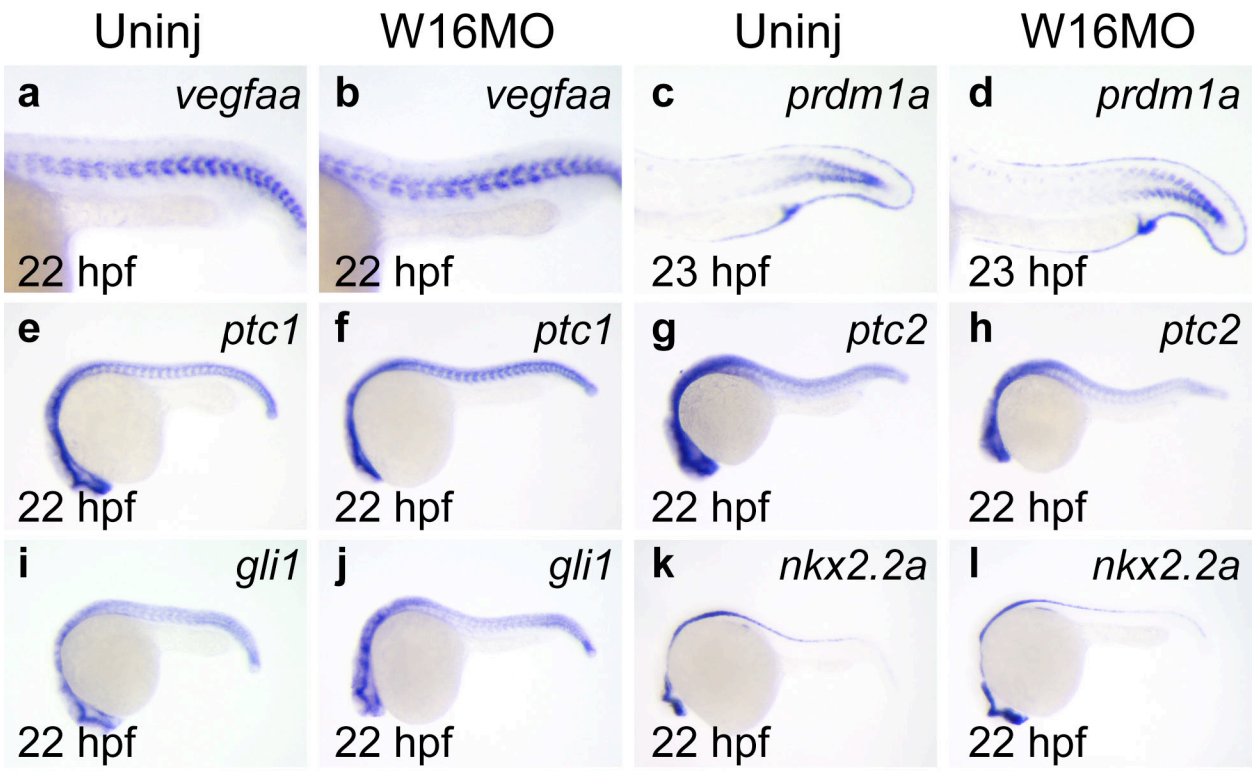

Supplementary Figure 14. Expression of Shh target genes in *wnt16* morphants. Expression of the indicated Shh target genes was examined in uninjected or W16MO-injected animals as indicated above each column, at the time points noted. No significant alteration was observed. a-d close up lateral views. e-l lateral views. All anterior to the left.

Figure S15

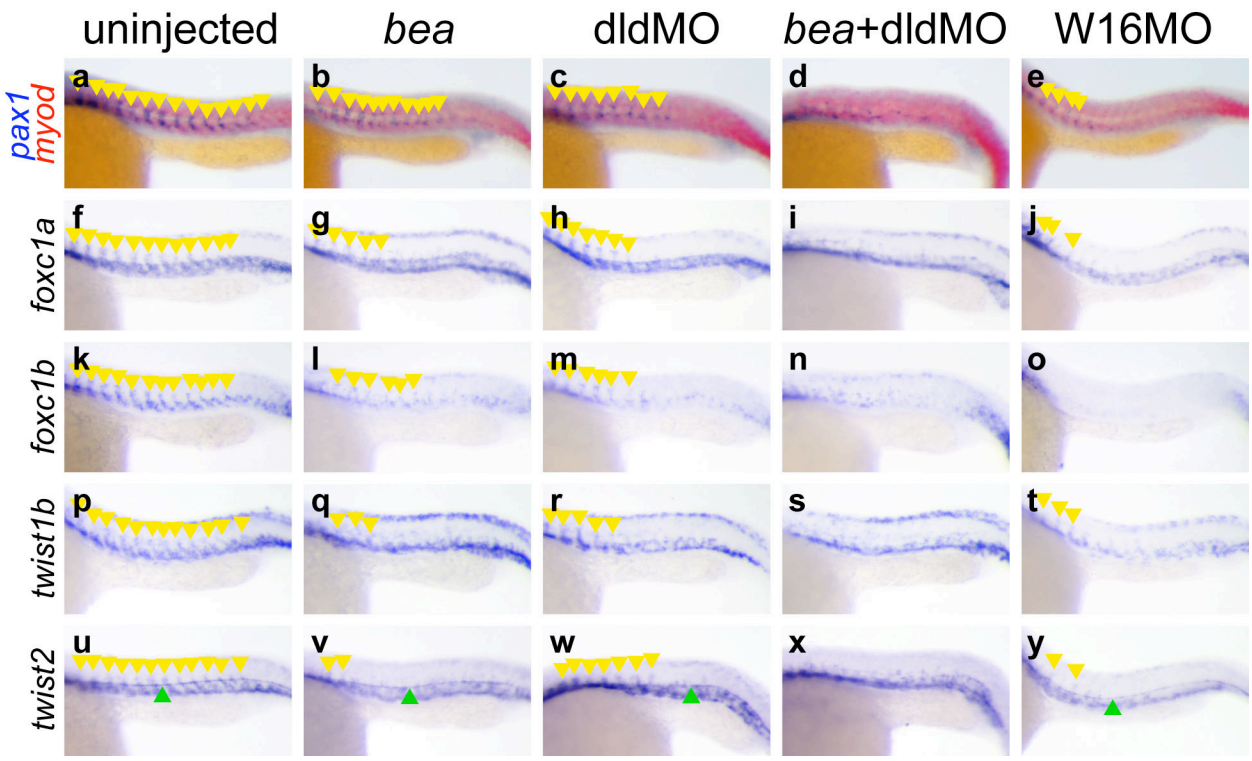

Supplementary Figure 15. Wnt16 and Dlc/Dld are required for sclerotome patterning. Expression of the sclerotomal markers *pax1* (a-e), *foxc1a* (f-j), *foxc1b* (k-o), *twist1b* (p-t), and *twist2* (u-y), with *myod* (a-d) shown for reference in red. Uninjected, homozygous *bea*, wild-type injected with dldMO, homozygous *bea* injected with dldMO, or W16MO embryos are shown as indicated above each column. Yellow arrowheads identify a dorsomedial somitic sclerotomal domain, when present. Green arrowheads identify the hypochord, when present (u-y). Close up lateral views of the trunk region, anterior left, dorsal up.

Supplementary Movie 1. HSCs in uninjected *cd41:GFP* transgenic animals. Timelapse imaging of the trunk region, where GFP^+ HSCs first appear near the dorsal aorta, in *cd41:GFP* transgenic animals visualized from approximately 50 hpf to approximately 75 hpf, at one frame every 3 mins. In the reference frames, red arrows indicate HSCs, and yellow arrows indicate multiciliate cells in the pronephros. Bright, rapidly circulating cells that begin appearing at about ~5 secs. (~53 hpf) are thrombocytes. Labelled reference frames have been added at 0 secs. (~50 hpf), 14 secs. (~60 hpf) and at 37 secs. (~75 hpf). Images were captured in parallel to the images presented in Movies S2-S4. Anterior to the left and dorsal up.

Supplementary Movie 2. HSCs are greatly reduced in W16MO-injected *cd41:GFP* transgenic animals. Timelapse images of W16MO-injected embryos, captured in parallel to the images presented in Movies S1, S3-S4, reveal vastly fewer HSCs, but normal multiciliate cells of the pronephros. Labelled as for Movie S1. Anterior to the left and dorsal up.

Supplementary Movie 3. Thymic immigration of lymphocyte precursors in *cd41:GFP* animals. Timelapse images of the head region of uninjected *cd41:GFP* transgenic animals captured in parallel to the images presented in Movies S1-S2, S4. The prospective thymus (50 hpf), thymic rudiment (60 hpf), and thymus (75 hpf) are identified with blue arrows in reference frames added at 0 secs., 14 secs., and 37 secs., respectively. Lymphocyte precursors retain the GFP label allowing visualization of their immigration. Anterior to the left and dorsal up.

Supplementary Movie 4. Greatly reduced thymic immigration of lymphocyte precursors in W16MO-injected *cd41:GFP* transgenic animals. Timelapse images of W16MO-injected embryos, captured in parallel to the images presented in Movies S1-S3, reveal vastly fewer lymphocyte precursors immigrating to the thymus. Labelled as for Movie S3. Anterior to the left and dorsal up.

Table S1. *Wnt16* mRNA overexpression effects.

Morphology	wild-type	dorsalized	A/P Defects[1]	Other
uninjected	232/235	0/235	0/235	3/235
70pg *wnt16s*	34/34	0/34	0/34	0/34
70pg *wnt16l*	28/199	18/199	140/199	13/199

chd at shield	wild-type	weak ectopic	strong ectopic
uninjected	81/81	0/81	0/81
70pg *wnt3*	0/38	4/38	34/38
70pg *wnt16l*	41/67	26/67	0/67
gfp at shield			
uninjected	34/34	0/34	0/34
70pg *wnt3*	0/20	0/20	20/20
70pg *wnt16l*	16/16	0/16	0/16
gfp at 16-s.			
uninjected	14/14	0/14	0/14
70pg *wnt16l*	18/18	0/18	0/18

[1]"A/P Defects" comprise anterior/posterior extension defects.

Table S2. W16MO effects on HSC-associated genes.

HSC Genes				
	treatment	wild-type	weak	strong
runx1[1]	Uninj	202/251	49/251	0/251
	5ng CoMO	8/13	5/13	0/13
	5ng W16MO	39/249	16/249	194/249
cmyb[1]	Uninj	96/109	13/109	0/109
	5ng CoMO	27/34	7/34	0/34
	5ng W16MO	27/116	26/116	63/116
cd41:GFP	Uninj	98/98	0/98	0/98
	5ng CoMO	121/125	4/125	0/125
	5ng W16MO	52/145	9/145	84/145
rag1[3]	Uninj	39/40	1/40	0/40
	5ng CoMO	12/12	0/12	0/12
	5ng W16MO	2/58	15/58	41/58

[1]"Wild-type" denotes abundant positive cells in the aortic region. "Weak" denotes intermediate decrease. "Strong" denotes very few or no positive cells. [2]"Wild-type" denotes abundant small round cells between the dorsal aorta and posterior cardinal vein. "Weak" denotes intermediate decrease. "Strong" denotes very few, or no positive cells. [3]"Wild-type" denotes strong bilateral thymic *rag1*$^+$ cells. "Weak" denotes decreased or one-sided *rag1*$^+$ cells. "Strong" denotes almost no, or no *rag1*$^+$ cells.

Table S3. W16MO effects on control genes.

Unaffected Genes				
	treatment	wild-type	weak	strong
gata1	Uninj	33/36	3/36	0/36
	5ng W16MO	49/49	0/49	0/49
myod	Uninj	29/29	0/29	0/29
	5ng W16MO	38/42	4/42	0/42
tll1	Uninj	49/49	0/49	0/49
	5ng W16MO	37/55	12/55	6/55
cdh5	Uninj	32/32	0/32	0/32
	5ng W16MO	17/17	0/17	0/17
flk1	Uninj	34/34	0/34	0/34
	5ng W16MO	31/31	0/31	0/31
efnb2a	Uninj	53/53	0/53	0/53
	5ng W16MO	55/55	0/55	0/55
col2a1a	Uninj	85/90	5/90	0/90
	5ng W16MO	72/79	7/79	0/79
cdh17	Uninj	30/30	0/30	0/30
	5ng W16MO	45/45	0/45	0/45
foxn1	Uninj	14/14	0/14	0/14
	5ng W16MO	0/9	0/9	0/9
shha	Uninj	20/20	0/20	0/20
	5ng W16MO	20/20	0/20	0/20
gfp	Uninj	102/102	0/102	0/102
	5ng CoMO	26/26	0/26	0/26
	5ng W16MO	73/73	0/73	0/73

[1]Some effects in this group may reflect heterochronicity. [2]WISH processing for *GFP* transcripts in *TOP:GFP* transgenic animals.

Table S4. W11MO effects on HSC genes.

Wnt11 Morpholino Phenotypes				
	treatment	wild-type	weak effect	strong effect
runx1	Uninj	19/20	1/20	0/20
	W11MO	25/29	4/29	0/29
cmyb	Uninj	20/20	0/20	0/20
	W11MO	9/16	7/16	0/16
cyclopia	Uninj	40/40	0/40	0/40
	W11MO	0/45	0/45	45/45

Table S5. W16MO and CoMO effects on Notch pathway genes.

Notch Pathway Genes				
	treatment	wild-type	weak	strong
dlc (16-18hpf)	Uninj	51/51	0/51	0/51
	5ng CoMO	24/27	3/27	0/27
	5ng W16MO	0/63	7/63	56/63
dlc (22-25hpf)	Uninj	113/114	1/114	0/114
	5ng CoMO	64/67	3/67	0/67
	5ng W16MO	134/174	30/174	10/174
dld (16-18hpf)	Uninj	76/76	0/76	0/76
	5ng CoMO	52/73	21/73	0/73
	5ng W16MO	20/120	47/120	53/120
dll4	Uninj	93/96	3/96	0/96
	5ng CoMO	30/36	6/36	0/36
	5ng W16MO	19/81	56/81	6/81
jag1b	Uninj	44/44	0/44	0/44
	5ng CoMO	35/35	0/35	0/35
	5ng W16MO	69/69	0/69	0/69
jag2	Uninj	28/28	0/28	0/28
	5ng CoMO	17/17	0/17	0/17
	5ng W16MO	35/35	0/35	0/35
notch1a	Uninj	28/28	0/28	0/28
	5ng CoMO	18/18	0/18	0/18
	5ng W16MO	34/34	0/34	0/34
notch1b	Uninj	145/145	0/145	0/145
	5ng CoMO	79/80	1/80	0/80
	5ng W16MO	134/191	41/191	19/191
notch2	Uninj	41/41	0/41	0/41
	5ng CoMO	17/17	0/17	0/17
	5ng W16MO	29/29	0/29	0/29
notch3	Uninj	150/154	4/154	0/154
	5ng CoMO	65/69	4/69	0/69
	5ng W16MO	155/207	39/207	13/207

Table S6. Notch path perturbation effects on HSC-associated genes.

HSC Genes				
		wild-type	weak	strong
runx1	uninj	99/111	12/111	0/111
	bea	12/68	44/68	12/68
	dldMO2	0/22	12/22	10/22
	bea+dldMO2	0/31	0/31	31/31
cmyb	uninj	62/67	5/67	0/67
	bea	11/60	32/60	16/60
	dldMO2	0/12	5/12	7/12
	bea+dldMO2	0/18	0/18	18/18
rag1	uninj	41/41	0/41	0/41
	bea	28/35	7/35	0/35
	dldMO2	27/28	1/28	0/28
	bea+dldMO2	0/9	0/9	9/9

Table S7. W16MO effects on Shh pathway genes.

Shh Target Genes				
	treatment	wild-type	weak	strong
vegfaa	Uninj	32/32	0/32	0/32
	5ng W16MO	42/53	11/53	0/53
prdm1a	Uninj	74/74	0/74	0/74
	5ng W16MO	56/56	0/56	0/56
ptc1	Uninj	62/62	0/62	0/62
	5ng W16MO	53/57	4/57	0/57
ptc2	Uninj	33/33	0/33	0/33
	5ng W16MO	36/36	0/36	0/36
gli1	Uninj	33/33	0/33	0/33
	5ng W16MO	44/44	0/44	0/44
nkx2.2a	Uninj	39/39	0/39	0/39
	5ng W16MO	50/50	0/50	0/50

Table S8. Notch rescue of W16MO HSC phenotype.

	wild-type	decreased	increased
uninj	27/33	6/33	0/33
uninj NICD+	2/11	0/11	9/11
W16MO NICD- 14h hs	9/73	63/73	2/73
W16MO NICD+ 14h hs	3/13	1/13	9/13
W16MO NICD- 16h hs	7/33	26/33	0/33
W16MO NICD+ 16h hs	4/14	10/14	0/14

Table S9. Loss of sclerotome in W16MO and Dlc/Dld Knock down.

Sclerotome Genes				
	treatment	wild-type	weak	strong
pax1	Uninj	160/165	3/165	2/165
	5ng CoMO	27/27	0/27	0/27
	5ng W16MO	4/155	39/155	117/155
	bea	13/67	50/67	4/57
	7ng dldMO	5/48	43/48	0/48
	bea+dldMO	0/52	10/52	42/52
foxc1a	Uninj	127/127	0/127	0/127
	5ng CoMO	14/14	0/14	0/14
	5ng W16MO	0/73	0/73	73/73
	bea	0/68	68/68	0/68
	7ng dldMO	13/68	53/68	2/68
	bea+dldMO	0/52	0/52	52/52
foxc1b	Uninj	92/92	2/94	0/94
	5ng CoMO	18/18	0/18	0/18
	5ng W16MO	0/91	0/91	91/91
	bea	0/32	32/32	0/32
	7ng dldMO	6/39	33/39	0/39
	bea+dldMO	0/34	2/34	32/34
twist1b	Uninj	55/55	0/55	0/55
	5ng CoMO	19/19	0/19	0/19
	5ng W16MO	0/41	8/41	33/41
	bea	0/16	16/16	0/16
	7ng dldMO	6/14	8/14	0/14
	bea+dldMO	0/37	0/37	37/37
twist2	Uninj	24/24	0/24	0/24
	5ng W16MO	0/23	5/23	18/23
	bea	0/18	0/18	18/18
	7ng dldMO	3/22	5/22	14/22
	bea+dldMO	0/17	0/17	17/17